ICES Journal of Marine Science

ICES Journal of Marine Science (2016), doi:10.1093/icesjms/fsw248

Solar UVR sensitivity of phyto- and bacterioplankton communities from Patagonian coastal waters under increased nutrients and acidification

Cristina Durán-Romero[1,*], Virginia E. Villafañe[1,2], Macarena S. Valiñas[1,2], Rodrigo J. Gonçalves[1,2], and E. Walter Helbling[1,2]

[1]*Estación de Fotobiología Playa Unión, Casilla de Correos N°15 (9103), Rawson, Chubut, Argentina*
[2]*Consejo Nacional de Investigaciones Científicas y Técnicas (CONICET), Argentina*

**Corresponding author: tel: +54 (280) 4498019; e-mail: cduran@efpu.org.ar.*

Durán-Romero, C., Villafañe, V. E., Valiñas, M. S., Gonçalves, R. J., and Helbling, E. W. Solar UVR sensitivity of phyto- and bacterioplankton communities from Patagonian coastal waters under increased nutrients and acidification. – ICES Journal of Marine Science, doi:10.1093/icesjms/fsw248.

Received 24 May 2016; revised 17 November 2016; accepted 14 December 2016.

The effects of ultraviolet radiation (UVR) under future expected conditions of acidification and increase in nutrient inputs were studied on a post-bloom phytoplankton and bacterioplankton community of Patagonian coastal waters. We performed an experiment using microcosms where two environmental conditions were mimicked using a cluster approach: present (ambient nutrients and pH) and future (increased nutrients and acidification), and acclimating the samples for five days to two radiation treatments (full solar radiation [+UVR] and exclusion of UVR [–UVR]). We evaluated the short-term (hours) sensitivity of the community to solar UVR through chlorophyll *a* fluorescence parameters (e.g. the effective photochemical quantum yield of PSII [Φ_{PSII}]) at the beginning, at the mid-point and at the end of the acclimation period. Primary production and heterotrophic bacterial production (HBP) were determined, and biological weighting functions were calculated, at the beginning and at the end of the acclimation period. Mid-term effects (days) were evaluated as changes in taxonomic composition, growth rates and size structure of the community. Although the UVR-induced inhibition on Φ_{PSII} decreased in both clusters, samples remained sensitive to UVR after the 5 days of acclimation. Also, under the future conditions, there was, in general, an increase in the phytoplankton carbon incorporation rates along the experiment as compared to the present conditions. Bacterioplankton sensitivity to UVR changed along the experiment from inhibition to enhancement of HBP, and future environmental conditions stimulated bacterial growth, probably due to indirect effects caused by phytoplankton. Those changes in the microbial loop functioning and structure under future global change conditions might have important consequences for the carbon pump and thus for the carbon sequestration and trophodynamics of Patagonian coastal waters.

Keywords: bacterioplankton, BWF, phytoplankton, production, PSII photochemistry.

Introduction

Many of the effects of global change are the result of the increase in greenhouse gases, mainly CO_2, derived from anthropogenic activities (Sabine *et al.*, 2004). Increases in atmospheric CO_2 cause a rise of the surface temperature (IPCC, 2013) with the concomitant stratification in aquatic systems towards shallower upper mixed layers (UMLs) (De Senerpont Domis *et al.*, 2013). This decrease of the UML will increase the exposure of planktonic organisms to solar radiation, including ultraviolet radiation (UVR, 280–400 nm). Also, increasing CO_2 dissolution leads to an alteration of the water chemical balance (Doney *et al.*, 2009) lowering the average pH of the ocean (pH expected value by 2100: 7.6; Gattuso *et al.*, 2010).

Changes in abiotic factors related to global change (i.e. UVR, temperature, pH, nutrients input, etc.) have important effects on planktonic organisms which constitute the base of the aquatic

trophic webs. In general, both ambient and increased levels of UVR cause deleterious effects on the phytoplankton and bacterioplankton physiology (e.g. Ruiz-González *et al.*, 2013; Häder *et al.*, 2015) although no effects and stimulatory effects have also been observed (Medina-Sánchez *et al.*, 2002; Gao *et al.*, 2007). UVR frequently interacts with other global change variables in a synergistic or antagonistic manner (Crain *et al.*, 2008). For example, higher nutrient availability may reduce the negative effects of UVR on phytoplankton (by improving the photochemical quantum yield of PSII, Marcoval *et al.*, 2007), and on bacterioplankton (by increasing heterotrophic bacterial production [HBP], Medina-Sánchez *et al.*, 2006). However, in some cases, higher nutrients availability results in an increase of the negative UVR effects, or in the unmasking of them which were not evident under nutrient limitation (Carrillo *et al.*, 2008; Ogbebo and Ochs, 2008). Different responses of phytoplankton have been documented under acidification conditions, as observed in the diatom *Thalassiosira pseudonana* that became more sensitive to UVR when grown under low pH (Sobrino *et al.*, 2008); on the other hand, acidification may also result in higher growth and production rates of diatoms exposed to UVR (Domingues *et al.*, 2014). Also acidification might alleviate the UVR-induced photoinhibition in the diatom *Chaetoceros curvisetus* (Chen *et al.*, 2014). In bacterioplankton, growth may be enhanced directly under higher acidification (through stimulation of hydrolytic enzymes) and indirectly (through increase in algal carbon excretion) (Allgaier *et al.*, 2008; Endres *et al.*, 2014). In addition, under high irradiances, HBP is stimulated under current ocean pH as compared with future acidification conditions (Mercado *et al.*, 2014).

In coastal systems (e.g. estuaries) there are more complex interactions with the various inputs [i.e. inorganic nutrients, dissolved organic matter (DOM), etc.] and abiotic factors which can affect the balance between primary production and respiration and hence the pH (Duarte *et al.*, 2013). Among these inputs, inorganic nutrient entry has become important in coastal ecosystems due to their increase via runoff from urban activities (Scavia *et al.*, 2002) and atmospheric deposition (Mahowald *et al.*, 2011). Also, by the end of the 21th century, the effects of acidification as a consequence of anthropogenic activities will exceed the natural causes in many estuaries (Cai *et al.*, 2011). Moreover, the alterations in global change variables are expected to have a profound impact in aquatic communities of estuaries and coastal areas as these sites provide an important share of the global production (Cloern *et al.*, 2014). This would be the case of areas such as the Atlantic Patagonian coast, which is highly productive in terms of fisheries (Skewgar *et al.*, 2007). In this area, several studies evaluated the impact of some global change variables on phytoplankton growth and photosynthesis (e.g. Marcoval *et al.*, 2008; Helbling *et al.*, 2015). Only one study (Villafañe *et al.*, 2015) considered the joint effects of UVR, nutrients enrichment and acidification on a post-bloom phytoplankton community, determining important taxonomic changes towards more UVR resistant species under simulated future conditions. In the case of bacterioplankton a previous study (Manrique *et al.*, 2012) determined that UVR had a key role in shaping the taxonomic composition of the community, but to our best knowledge there are no studies that evaluated the combined effects of several global change variables on these communities.

To address this gap of knowledge and to gain a better understanding on the impact of global change variables on planktonic communities of the Patagonian area, we designed a "cluster type" experiment (Boyd *et al.*, 2010; Villafañe *et al.*, 2015) to assess the combined effects of increased nutrients and acidification under solar UVR on production and size structure of summer phyto- and bacterioplankton. Particularly, we asked whether the simultaneous action of increased inorganic nutrient availability and lower pH, as expected in the future, would interact to influence the effects of UVR on these communities and if so, to what extent. In this study, we went a step further in the knowledge by providing a fine detail of the effects of different wavebands i.e. by determining biological weighting functions (BWFs; Neale and Kieber, 2000) for phytoplankton and bacterioplankton production under the present and an expected future scenario of global change (in terms of nutrients input and acidification).

Methods

Study site

Water sample for incubation was collected from the seawater end point of the Chubut River estuary (Patagonia, Argentina, 43° 20.5′S, 65° 02.0′W) at Egi station (ca. 1000 m away from the shore). Previous studies have described the phytoplankton seasonal succession in this site, which consists of a winter bloom of diatoms (>20 μm) and the dominance of pico-nanoplankton species (<20 μm) during spring and summer (Villafañe *et al.*, 2004). This area is characterized by relatively high phytoplankton biomass associated with nutrient inputs from anthropogenic origin carried by the river (Helbling *et al.*, 1992, 2010). Macronutrient concentrations in the Chubut River estuary range from 0.20 to 21 μM for nitrate (NO_3^-), 0.19–6.40 μM for phosphate (PO_4^{3-}), and 1.70–236 7 μM for silicate (SiO_3^{2-}) (Helbling *et al.*, 2010), with very little or almost null concentrations of ammonia ($NH4^+$) (Häder *et al.*, 2015). Significant variations in the penetration of solar radiation have also been reported, with the attenuation coefficient for photosynthetic active radiation (k_{PAR}—PAR, 400–700 nm) ranging from <1 to >4 m^{-1} during high and low tides, respectively. Mean water temperature ranges from 19 °C in summer to 4 °C in winter (Helbling *et al.*, 2010) whereas pH values range between 8.03 and 8.32 throughout the year (P. Bermejo, pers. comm.).

Experimental setup

The experiment was conducted from 2 to 6 February 2015, and the experimental setup consisted of two phases:

Phase 1 (acclimation), in which the samples were exposed in microcosms for 5 days (starting on 2 February 2015) to two environmental conditions (referred to as Present and Future clusters) and two radiation treatments (i.e. +UVR and −UVR) (see below).

Phase 2, short-term (<1 day) determinations, that consisted of: (i) daily cycles (i.e. from sunrise to sunset) of measurements of fluorescence parameters, done at the initial, middle and final days of the acclimation phase, and (ii) phytoplankton and bacterial production using BWFs (see below) done at the initial and final days of the acclimation phase. Previous studies of our group in the area showed that an acclimation of 5 days was enough to detect changes in species composition as well as in other acclimation mechanisms such as UV-absorbing compounds (e.g. Marcoval *et al.*, 2008). Another study about the interactive effects of acidification and radiation used similar incubation times (Domingues *et al.*, 2014) taking into account that the acclimation to environmental changes occurs in a few days (Satoh *et al.*,

2001). Two contrasting environmental conditions (the above mentioned clusters) were tested: (i) Present: Samples with *in situ* nutrients concentration (i.e. 2.02, 1.42, and 28.70 μM of nitrate + nitrite, phosphate, and silicate, respectively) and pH = 8.20, (ii) Future: Samples with increased nutrients concentration and lower pH values (pH = 7.65, Gattuso *et al.*, 2010) to meet levels expected by the end of the century (IPCC, 2013). Increased nutrients concentration was achieved by adding macronutrients to reach values of NO_3^-: 60.32 μM, PO_4^{3-}: 28.18 μM and SiO_3^{2-}: 218.65 μM mimicking a higher input of nutrients from the Chubut river due to human activity (Depetris *et al.*, 2005) and also an increase in wind deposition (England *et al.*, 2014) and rain (IPCC, 2013). To lower the pH, CO_3^{2-} (as Na_2CO_3), HCO_3^- (as $NaHCO_3$) and HCl (0.01N) were added to the seawater to increase the pCO_2 and the content of dissolved inorganic carbon (DIC) as recommended by Gattuso *et al.* (2010) and Yates *et al.* (2013). We chose to manipulate the water pH by this method rather than by CO_2 bubbling, in order to avoid the indirect effects of the bubbling turbulence such as the promotion of coagulation of organic matter, thus affecting microbial interactions (Burrell *et al.*, 2016), or the effects on growth of several phytoplankton species (Shi *et al.*, 2009). Surface seawater was collected with an acid-cleaned bucket (1N HCl) late in the evening of the previous day of the start of the experimentation, and immediately taken to the laboratory at Estación de Fotobiología Playa Unión (EFPU, 10 min away from the harbour). While setting up the experiment, the water was maintained at 19°C in darkness. The water sample was pre-screened (200 μm mesh) to remove large zooplankton, and put into two acid-cleaned (1N HCl) containers (10 l) so that one of them was kept at the present environmental condition whereas the other was manipulated as mentioned above to represent the future condition. Each 10-l container was subsequently divided into 6 microcosms that consisted of 500 ml UVR-transparent screw cap-Teflon bottles [the spectra transmission was published in Villafañe *et al.* (2015)]. The microcosms were exposed outdoors under the two radiation treatments mentioned above (+UVR and –UVR): For each environmental condition, 3 microcosms received PAR + UVR (+UVR; full solar radiation; >280 nm; uncovered bottles), while the other 3 received only PAR (−UVR, >400 nm; bottles covered by UVR-opaque film Ultraphan 395). The 12 microcosms (i.e. 6 present and 6 future) were placed inside a water bath (10 cm depth) receiving an homogeneous radiation field, without shadows from the walls, with controlled temperature (19 ± 1 °C) during daytime. The whole initial set up lasted around 2 h and ended after sunset, so that the samples did not receive any solar radiation until the following morning when the measurements started. The microcosms were gently shaken every hour during daylight to avoid the settlement of cells and to warrant homogeneous irradiance inside the bottles.

The plankton communities were maintained in semi-continuous growth, with half of the volume (250 ml) of the microcosms replaced daily (early in the morning before the samples received any solar radiation) with filtered (GF/F) and sterile seawater collected at the same time of sampling. The sterile seawater was kept at 19 °C in darkness and had the same physical-chemical characteristics as the present conditions; in the case of the future conditions, nutrients and acidification were increased just before being added to the microcosms to reach the same levels mentioned above for this condition. The removed 250 ml were used to determine chlorophyll *a* (Chl-*a*) concentration (daily measurements) and fluorescence parameters of the photosystem II [days 1 (t_1), 3 (t_3), and 5 (t_5)], abundance of phytoplankton and bacterioplankton (daily determinations), phytoplankton carbon incorporation, and HBP (days 1 and 5) as explained below.

Chemical characterization and pH measurements

The initial nutrients concentrations (nitrate + nitrite, phosphate and silicate) in the present and future environmental clusters were determined at the start of the incubations using a scanning spectrophotometer (Hewlett Packard, model 8453E, USA) as described in Strickland and Parsons (1972). The pH was measured daily using a pH meter (Hanna Instruments, model HI 2211, USA) and adjusted every day (following the procedure explained earlier) according to the requirement of each microcosm to keep an average pH value of 7.65 in the future condition.

Solar radiation

Solar radiation over the study area was measured continuously using a broad-band European Light Dosimeter Network radiometer (Real Time Computers, Germany) permanently installed on the roof of the EFPU. This instrument measures irradiance in the UV-B (280–315 nm), UV-A (315–400 nm), and PAR ranges and stores the minute-averaged values. This radiometer is calibrated yearly using a solar calibration procedure.

Chl-*a* fluorescence parameters

Chl-*a* fluorescence parameters were measured throughout daily cycles i.e. from sunrise to sunset (8 a.m. to 7 p.m.) at the beginning (2 February, t_1), at the middle (4 February, t_3) and at the end of the acclimation phase (6 February, t_5). Sub-samples (50 ml) from each microcosm were put in quartz tubes and maintained under the same irradiance conditions as in the microcosms (i.e. +UVR and –UVR). For these daily cycles, one aliquot (2 ml) from each tube was collected every hour to determine the effective photochemical quantum yield (Φ_{PSII}) as well as other fluorescence parameters using a portable pulse-amplitude modulated fluorometer (Walz, model Water-ED PAM, Germany). For each of these sub-samples, Φ_{PSII} values were obtained six consecutive times by measuring the instant maximum fluorescence (F'_m) induced by a saturating pulse (~5300 μmol photons m^{-2} s^{-1} in 0.8 s) and the steady state fluorescence (F_t) induced by an actinic light (ca. 500 μmol photons m^{-2} s^{-1}) in light-adapted cells. The light source consists of light emitting diodes peaking at 650–660 nm. Calculations of Φ_{PSII} followed the equations of Genty *et al.* (1989) as:

$$\Phi_{PSII} = \Delta F/F'_m = (F'_m - F_t)/F'_m \quad (1)$$

To quantify the decrease and the increase in Φ_{PSII} (inhibition and recovery, respectively) during the daily cycles, we fit an exponential function to the Φ_{PSII} values during the day as a function of time (Equation 2):

$$\Phi_{PSII} = A\ e^{bt} \quad (2)$$

where A is a constant, t is the time (minutes) and b represents the rate of change. When this rate was negative we considered it as *inhibition* (*k*, in min^{-1}) whereas if it was positive we considered it as *recovery* (*r*, in min^{-1}). Thus higher absolute values mean either higher inhibition (negative sign) or recovery (positive sign) rates. We considered the measurements from 8 a.m. until the moment

in which Φ_{PSII} stopped decreasing (ca. local noon) to determine k, and the measurements in which Φ_{PSII} constantly increased until 7 p.m. for r.

Biological weighting functions

The phytoplankton and bacterioplankton carbon incorporation under five UVR different wavelength intervals were expressed as a function of the average irradiance (over the incubation time) in the wavelength exposure intervals (i.e. BWFs; Rundel, 1983). Mean BWFs for carbon incorporation in phytoplankton (BWF_{phyto}) were calculated at the beginning of the experiment for both environmental conditions (present and future), and at the end of the acclimation phase for the present and future conditions as well as for the radiation treatments (+UVR and −UVR). The samples were dispensed in 30 ml UVR-transparent Teflon bottles, inoculated with radiocarbon (0.185 MBq of labelled sodium bicarbonate) and incubated under solar radiation in a water bath at the same temperature as the microcosms for 2 h around noon. Six different radiation treatments were obtained, using Schott cut-off filters [WG280, WG295, WG305, WG320, WG360, and GG400, the spectral transmission of these filters was published in Villafañe *et al.* (2003)], in order to obtain five wavelength intervals: 280–295; 295–305; 305–320; 320–360; and 360–400 nm. BWF_{phyto} were calculated using an exposure–response curve based on the irradiance (Neale, 2000). The biological response for each wavelength interval was expressed as a function of the average irradiance during the exposure interval and normalized to 1 at 300 nm. The irradiance in each wavelength interval was obtained with a USB diode array spectroradiometer (Ocean Optics, model HR 2000CG-UV-NIR, USA) attached to a 10 m fibre optics cable and a cosine-corrected sensor. A third degree polynomial function was fitted to the data from each experimental series; the best fit was then obtained by iteration ($R^2 > 0.95$) (Buma *et al.*, 2009). Due to space restrictions under the Schott filters to fit all the Teflon bottles, at the end of the acclimation period the samples were incubated in two consecutive sets, separating those samples acclimated to +UVR and –UVR; however these two sets of incubations were done under similar solar irradiances (as both incubations were performed around local noon).

After the incubation period, the samples were filtered onto glass fibre filters (Whatman GF/F, 25 mm) under low vacuum (<100 mm Hg); the filters were placed into 5 ml scintillation vials, and exposed to HCl fumes overnight to remove the inorganic carbon (i.e. not incorporated by phytoplankton). After acidification, scintillation cocktail (Optiphase Hisafe 3, Perkin Elmer) was added to the vials and the carbon incorporated was determined from the counts (Holm-Hansen and Helbling, 1995).

Mean BWFs for HBP (BWF_{bact}) were also obtained at the beginning and at the end of the acclimation phase. The water used to determine BWF_{bact} was that not retained by the GF/F filter during the filtrations performed for BWF_{phyto} (see above); thus this water contained cells < 0.7 μm that were already exposed to the different radiation treatments under the Schott filters for 2 h as explained earlier for BWF_{phyto}. HBP in these samples already exposed under the Schott filters was determined in the dark by using ^{3}H-Leucine (specific activity = 52.9 Ci mmol^{-1}, Amersham Pharmacia) incorporation as a direct measurement of carbon production (Simon and Azam, 1989). ^{3}H-Leucine was added to sterile microcentrifuge tubes with 1.5 ml of sample (three replicates and one trichloroacetic acid [TCA]-killed control per treatment) to reach a final saturating concentration of 40 nM. The tubes with the radiotracer were incubated (1 h) in darkness. After the incubation, the incorporation of ^{3}H-Leucine was stopped with 5% (final concentration) of TCA. Blanks were killed with TCA before the addition of the radiotracer. Extraction was performed with cold TCA, following Smith and Azam (1992). Finally, scintillation liquid (Optiphase Hisafe 3, Perkin Elmer) was added for subsequent measurements in a scintillation counter. The conversion factor 1.55 kg C mol^{-1} (Simon and Azam, 1989) was used to estimate the carbon produced per mol of incorporated ^{3}H-Leucine. Data of BWF_{bact} were expressed either as enhancement (when HBP was increased) or inhibition (when HBP was inhibited). Our data were also compared with those obtained by Wilhelm and Smith (2000) that were also based on leucine incorporation.

Phytoplankton and bacterioplankton abundance

Cell abundances were determined every day in each microcosm. Samples for identification and enumeration of phytoplankton (>2 μm) were put in 40-ml brown glass bottles and fixed with buffered formalin (final concentration 0.4% of formaldehyde). Sub-samples were stained with Rose Bengal and settled for 24 h in 10 ml-Uthermöl chambers (Hydro-Bios GmbH, Germany). Phytoplankton was counted and identified using an inverted microscope (Leica, model DM IL, Germany). Cell sizes were obtained from image analysis (100 images per replicate) by using ImageJ software 1.49p (National Institutes of Health, USA).

Autotrophic picoplankton (<0.7 μm) and bacterioplankton abundances were determined using flow-cytometry (FACScanto II, Becton Dickinson Biosciences, Oxford, UK) from samples filtered through Whatman GF/F filters (25 mm diameter) (three replicates and one control for each condition/treatment). Samples were fixed with 1% paraformaldehyde and stained with SYBR Green I DNA stain (Sigma-Aldrich) to a 1:5000 final dilution of the initial stock (Zubkov *et al.*, 2007). Yellow-green 1-μm beads (Fluoresbrite Microparticles, Polysciences, Warrington, PA, USA) were used as an internal standard of particle concentration and fluorescence (Zubkov and Burkill, 2006). Bacterioplankton cells were discriminated on bivariate plots of particle side scatter versus green fluorescence.

The specific growth rates (μ, in d^{-1}) of phytoplankton and bacterioplankton were calculated as follows:

$$\mu = \ln (N_f/N_0)/t \quad (3)$$

$$N_{(t)} = N_0 e^{kt} \quad (4)$$

where N_f and N_0 are phytoplankton or bacterioplankton abundances at the end and at the beginning of the experiment, respectively, t is the time (in days) between collection of samples, $N_{(t)}$ is the cell abundance at a particular time, and k represents the rate of change.

Chl-*a* concentration

Every day, samples (50 ml) from each microcosms were filtered onto Whatman GF/F filters (25-mm diameter) and frozen (−20 °C) until analysis. For Chl-*a* analyses, samples were thawed and placed in centrifuge tubes (15 ml) with 5 ml of absolute

methanol (Holm-Hansen and Riemann, 1978) and measured by fluorometric techniques (Holm-Hansen *et al.*, 1965) with a fluorometer (Turner Designs, model Trilogy, USA).

Statistical analysis

Two-way repeated measures ANOVAs (RM-ANOVA) were used to determine significant interactions among solar radiation treatments and environmental clusters conditions for inhibition (k) and for recovery (r) rates along the experiment. Two-way ANOVAs were used to determine interactions among solar UVR exposure and environmental clusters conditions on phytoplankton and on bacterioplankton production at the beginning of the experiment. Three-way ANOVAs were used to determine the interactive effects of short-term solar UVR exposure, solar radiation acclimation (i.e. +UVR and -UVR) and environmental clusters on phytoplankton and bacterioplankton production at the end of the acclimation phase. In order to determine the effects of the acclimation conditions on the specific growth rates of the different phytoplankton groups (diatoms, dinoflagellates, and flagellates), a three-way ANOVA was used, with radiation acclimation, environmental cluster and taxonomic group as factors. A two-way ANOVA was used to determine the interactive effects of radiation acclimation and environmental cluster on bacterioplankton growth rates. A t-test was used to determine significant differences between present and future conditions at day 1 in the UVR inhibition of phytoplankton and bacterioplankton production.

A post hoc Fisher LSD-test was used to identify which treatments (or dates) were significantly different. Data were checked for normality using the Kolmorov Smirnov test, while homoscedasticity was verified with Levene tests (Zar, 1999). When necessary, data were transformed to fit the assumptions of parametric tests; also, when necessary, error propagation was used.

Results

Solar irradiance conditions

The mean daily irradiances received by the microcosms during the experimental period were 0.64 ± 0.21, 22.30 ± 6.92, and 165 ± 54.89 W m^{-2} for UV-B, UV-A, and PAR, respectively. The mean daily doses for this period were 34, 1185 and 8794 kJ m^{-2}, for UV-B, UV-A, and PAR, respectively. In general, clear skies prevailed but some overcast was observed on 4 February.

Daily variations of the photochemical quantum yield

The daily variations of Φ_{PSII} (expressed as % of the initial Φ_{PSII}) showed similar trends under all treatments and dates (Figure 1), with an initial decrease as soon as the exposure started and then recovering during the afternoon. In all cases the recovery at the end of the day was only partial as the Φ_{PSII} percentages were lower than 100%. Based on the daily cycles of Φ_{PSII}, we calculated the inhibition (k) and recovery (r) rates for each environmental condition and treatment (Figure 2). There were no significant interactive effects of radiation treatment × environmental conditions × date on k and r, although there were significant effects of date × radiation treatment, and date × environmental conditions on k and r respectively (Table 1). The inhibition (k) decreased significantly from the beginning of the experiment towards the end of the acclimation phase (Figure 2). It is interesting to note that at the start of the acclimation phase (t_1), when samples were not yet exposed to solar radiation in our experimental conditions, samples receiving UVR (Figure 2a) were significantly more inhibited than those receiving only PAR (−UVR—Figure 2b). However, as the acclimation phase progressed, there were no significant differences between radiation treatment/environmental conditions in the inhibition of Φ_{PSII}. For recovery (r) we did not find a clear trend along the experiment.

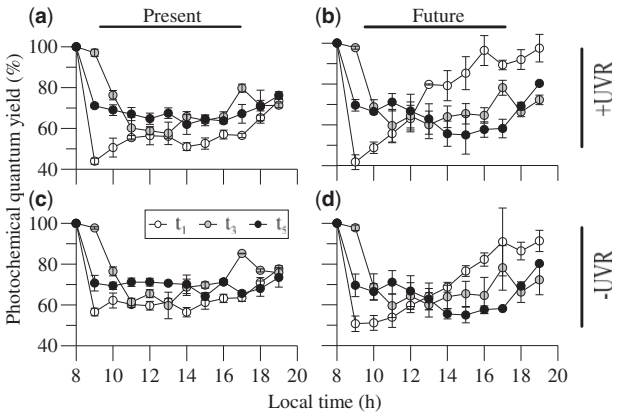

Figure 1. Daily cycles of the effective photochemical quantum yield (percentage of initial values of the day) of samples acclimated and exposed to full solar radiation (+UVR) or only PAR (−UVR) under present or future conditions on 2 (t_1), 4 (t_3), and 6 (t_5) February 2015. The symbols represent the mean values and the lines are the s.d. ($n = 3$).

Phytoplankton carbon incorporation

The detailed wavelength dependence of the short-term effects of solar UVR on phytoplankton carbon incorporation, assessed using BWFs (BWF_{phyto}) is shown in Figure 3. Solar UV-B had a greater impact (i.e. higher biological weights) than UV-A and PAR, for all treatments and experimental days. The radiation effects of the different wavelengths were similar for both environmental conditions at the beginning of the experiment (Figure 3a). At the end of the acclimation phase, however, the sensitivity of phytoplankton decreased (Figure 3b), with samples under the present condition having the lowest (+UVR_{pre}) and the highest (−UVR_{pre}) sensitivity within the UV-A region of the spectrum. In the samples under the future condition the differences in sensitivity were smaller among radiation treatments (i.e. +UVR_{fut} and −UVR_{fut}) at the end of the acclimation phase (Figure 3b). Samples in the present condition, and acclimated to +UVR, were the most sensitive under the lowest wavebands of UV-B, having the highest biological weights.

In order to assess the overall short-term impact of solar UVR on phytoplankton carbon incorporation, we compared the carbon incorporation rates of samples receiving the full solar radiation spectrum—UVR + PAR (i.e. under WG280 filter)—with those exposed only to PAR (i.e. under GG400 filter) (Figure 4). There were no significant interactive effects between radiation treatment and environmental conditions at the beginning (Figure 4a; Table 2), or among solar short-term UVR exposure, environmental conditions and acclimation to solar radiation treatments at the end of the experimental period (Table 2). There were, however, significant single effects of solar UVR inhibiting carbon incorporation rates at the beginning of the experiment (Figure 4a) in both the present and future conditions. This inhibition of the initial sample was significantly higher (t-test, $p < 0.05$) in the

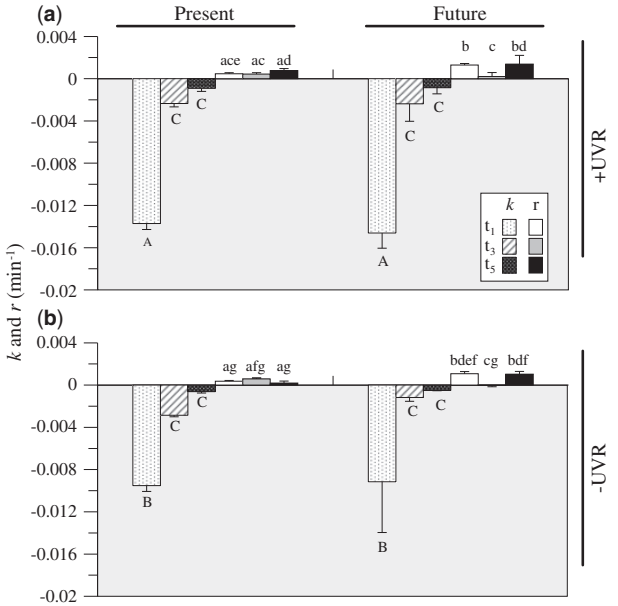

Figure 2. Inhibition (*k*, negative values) and recovery (*r*, positive values) rates (in min^{-1}) of phytoplankton during the daily cycles of samples acclimated and exposed to full solar radiation (+UVR) or only PAR (−UVR) under present or future conditions on 2 (t_1), 4 (t_3), and 6 (t_5) February 2015. The values are the mean and the s.d. ($n = 3$). For inhibition, significant differences among treatments are denoted by capital letters, whereas for recovery, significant differences among treatments are denoted by lower case letters.

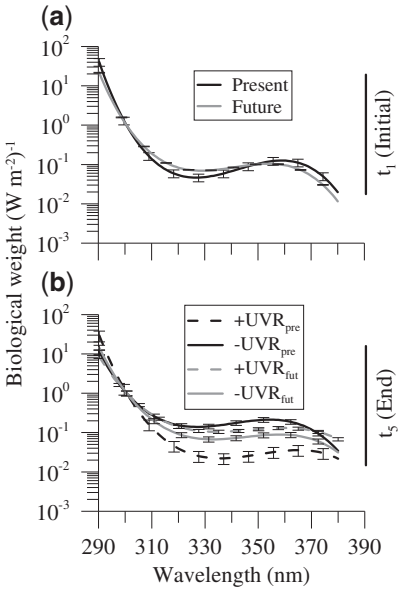

Figure 3. Mean BWF_{phyto} exposed to natural solar radiation under six spectral treatments and two environmental conditions [present (pre) vs. future (fut)]. (a) 2 February (Initial, t_1), samples without pre-acclimation. (b) 6 February (End, t_5), samples pre-acclimated with UVR (+UVR) or without UVR (−UVR) under present and future environmental conditions. Biological weights are expressed in $(W\ m^{-2})^{-1}$; the BWF data are normalized to 1 at 300 nm. The lines are the results of the model output, while the vertical lines indicate the 95% confidence limits of the model.

Table 1. Results from the two-way RM-ANOVA of the interactive effects among solar radiation treatment (Rad), environmental cluster (Env) and date on inhibition (*k*), and recovery rates (*r*) of the effective photochemical quantum yield.

			k		*r*	
	df1	**df2**	$F_{df1,df2}$	***P***	$F_{df1,df2}$	***p***
Env	1	8	0.36	0.561	9.07	**0.016**
Rad	1	8	19.15	**0.002**	3.47	0.099
Env × Rad	1	8	0.29	0.605	0.13	0.730
Date	2	16	121.59	**<0.001**	15.66	**<0.001**
Date × Env	2	16	0.51	0.609	19.53	**<0.001**
Date × Rad	2	16	16.06	**<0.001**	2.09	0.156
Date × Env × Rad	2	16	0.09	0.918	1.02	0.382

Numbers in bold indicate significant effect on the variable considered.

present, with a decrease of ca. 1.44 ± 0.32 pg C $cell^{-1}$ h^{-1}, as compared to the future condition, that had a decrease of ca. 0.91 ± 0.17 pg C $cell^{-1}$ h^{-1}. At the end of the experimental period (Figure 4b), acclimation to full solar radiation (+UVR) resulted in a significant decrease of the UVR inhibition, with values of 32.69 ± 8.16 and 40.35 ± 10.66% for the present and future conditions, respectively, as compared with the values of 74% (± 3.92) at the beginning of the experiment. In samples acclimated to −UVR, the UVR inhibition values were 70.26 ± 6.30 and 58.11 ± 14.08% for the present and future conditions, respectively. The lowest carbon incorporation rate at the end of the experiment was observed in the present condition, in samples acclimated to −UVR that was then exposed to the full solar radiation spectrum (Figure 4b).

Phytoplankton size structure and growth

The initial water sample had a Chl-*a* concentration of 3.26 μg l^{-1}, with a phytoplankton abundance of 15 × 10^3 cells ml^{-1}, dominated (ca. 98%) by unidentified flagellates (<10 μm). At the end of the experiment, the community was still dominated by flagellates in all treatments, although their dominance (i.e. % of the total cell abundance) decreased as compared to the initial community, while that of diatoms increased (Figure 5a). These differences in the relative dominance between diatoms and flagellates were also observed in the specific growth rates (μ—Figure 5b) with diatoms having higher μ than that of flagellates and dinoflagellates under all treatments. Under the present conditions there were no significant differences in μ between acclimations to solar radiation for any of these groups, whereas under the future condition, the μ of diatoms and flagellates were higher under the +UVR than under the −UVR acclimation (Figure 5b). There was no interactive effect of environmental conditions × radiation treatments × taxonomic group on phytoplankton growth rates, although there was a significant interactive effect between environmental conditions and radiation treatments (Table 3). Also, and at the end of the experiment, there was a shift towards smaller cells with area 5–20 μm^2 in samples acclimated to +UVR in the future condition, while in the other cases there was little change in the size structure of the community (Figure 5c).

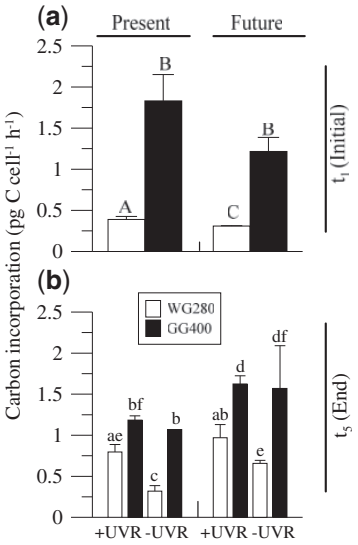

Figure 4. Phytoplankton carbon incorporation rates (in pg C cell^{-1} h^{-1}) during short-term exposures of samples to UVR (full solar radiation; under Schott filter WG280) or only to PAR (under Schott filter GG400). (a) 2 February (Initial, t_1), samples without pre-acclimation. (b) 6 February (End, t_5), samples pre-acclimated with UVR (+UVR) or without UVR (−UVR) under present and future environmental conditions. The values are the mean and the s.d. ($n = 3$). Significant differences among treatments on initial day are denoted by capital letters whereas at the end of the experiment they are denoted by lowercase letters.

Table 2. Results from the two-way (2 February; t_1) and the three-way (6 February; t_5) ANOVA of the interactive effects among short-term solar radiation exposure treatment (Rad), environmental cluster (Env), and acclimation to solar radiation (UVR) on phytoplankton and bacterioplankton carbon incorporation.

			Phytoplankton		**Bacterioplankton**	
t_1	**df1**	**df2**	**$F_{df1,df2}$**	***p***	**$F_{df1,df2}$**	***p***
Env	1	8	28.350	**<0.001**	8.29	**0.020**
Rad	1	8	643.91	**<0.001**	375.81	**<0.001**
Env×nv0	1	8	4.56	0.065	33.99	**<0.001**
t_5	**df1**	**df2**	**$F_{df1,df2}$**	***p***	**$F_{df1,df2}$**	***p***
Env	1	16	28.85	**<0.001**	15.56	**0.001**
UVR	1	16	20.79	**<0.001**	6.90	**0.018**
Rad	1	16	107.78	**<0.001**	22.64	**<0.001**
Env × UVR	1	16	1.98	0.178	0.70	0.416
Env × Rad	1	16	0.01	0.931	1.76	0.203
UVR × Rad	1	16	10.57	**0.005**	0.54	0.472
UVR × Env × Rad	1	16	1.31	0.268	0.00	0.954

Numbers in bold indicate significant effect on the variable considered.

Heterotrophic bacterial production

At the beginning of the experiment (Figure 6a) UVR had an inhibitory effect on HBP, showing a similar pattern than the BWF obtained by Wilhelm and Smith (2000) (lines 1 and 2). The inhibitory effect in the UV-A wavelengths was higher under the future than under the present condition (Figure 6a) whereas similar weights for both environmental conditions were obtained for the

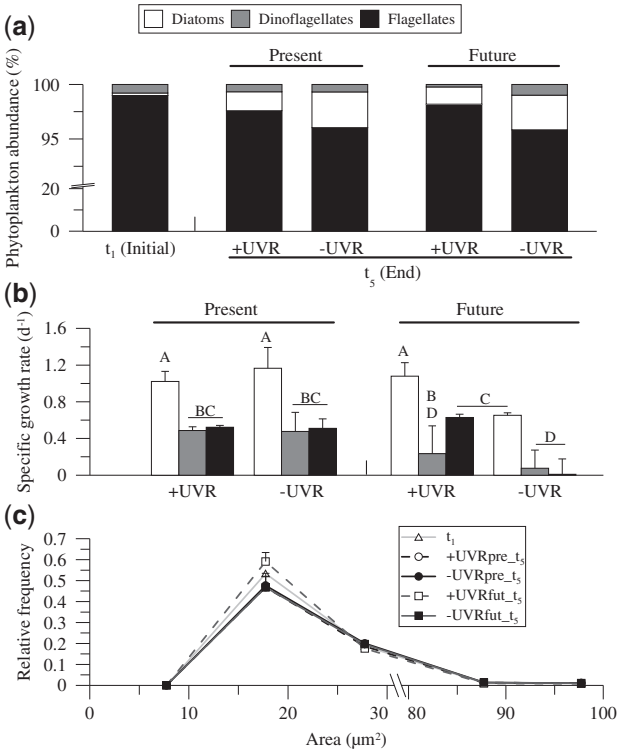

Figure 5. Changes in the phytoplankton community structure along the experiment. (a) Percentages abundance of diatoms (white bars), dinoflagellates (grey bars) and flagellates (black bars) on 2 February (Initial, t_1) and on 6 February (End, t_5) after acclimation with UVR (+UVR) or without UVR (−UVR) under present and future conditions. (b) Specific growth rates (d^{-1}) of diatoms (white bars), dinoflagellates (grey bars) and flagellates (black bars) acclimated to +UVR and −UVR under present and future conditions. The values are the mean and the s.d. ($n = 3$). Significant differences among treatments are denoted by capital letters. (c) Relative frequency of particle sizes (in µm^2) at the initial (t_1) and final day of experimentation (t_5). The symbols represent mean values and error bars represent the s.d. ($n = 3$).

Table 3. Results from the three-way (phytoplankton) or two-way ANOVA (bacterioplankton) of the interactive effects among acclimation to solar radiation (UVR), environmental cluster (Env), and group (in the case of phytoplankton: diatoms, flagellates or dinoflagellates), on the specific growth rate of phytoplankton and bacterioplankton based on cell abundance.

		df1	**df2**	**$F_{df1,df2}$**	***p***
Phytoplankton					
	Env	1	12	14.93	**0.002**
	UVR	1	12	7.83	**0.016**
	Group	2	12	40.25	**<0.001**
	Env × UVR	1	12	11.65	**0.005**
	Env × Group	2	12	0.36	0.703
	UVR × Group	2	12	1.15	0.348
	Env × Rad × Group	2	12	1.29	0.310
Bacterioplankton					
	Env	1	8	102.19	**<0.001**
	UVR	1	8	4.05	0.078
	Env × UVR	1	8	9.59	**0.014**

Numbers in bold indicate significant effect on the variable considered.

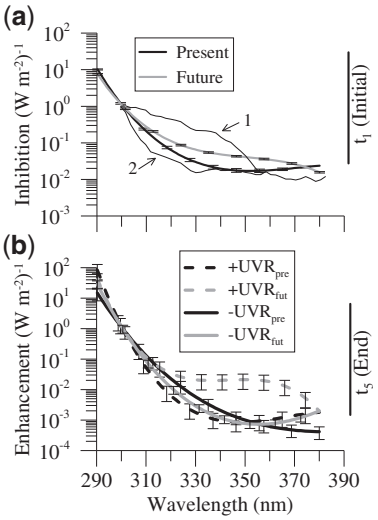

Figure 6. Mean BWF_{bact} exposed to natural solar radiation under six spectral treatments and two environmental conditions [present (pre) vs. future (fut)]. (a) 2 February (Initial, t_1), samples without pre-acclimation (expressed as inhibition). (b) 6 February (End, t_5), samples acclimated with UVR (+UVR) or without UVR (−UVR) under present and future environmental conditions (expressed as enhancement). Biological weights are expressed in $(W\ m^{-2})^{-1}$; the BWF data are normalized to 1 at 300 nm. The lines are the results of the model output, while the vertical lines indicate the 95% confidence limits of the model. Lines 1 and 2 are the BWFs calculated from data published in Wilhelm and Smith (2000).

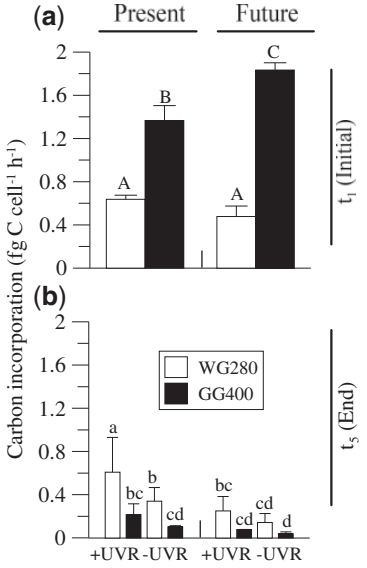

Figure 7. Bacterioplankton productivity (in fg C $cell^{-1}$ h^{-1}) during short-term exposures of samples to UVR (full solar radiation; under Schott filter WG280) or only to PAR (under Schott filter GG400). (a) 2 February (Initial, t_1), samples without pre-acclimation. (b) 6 February (End, t_5), samples acclimated with UVR (+UVR) or without UVR (−UVR) under present and future environmental conditions. The values are the mean and the s.d. ($n = 3$). Significant differences among treatments on initial day are denoted by capital letters whereas at the end of the experiment they are denoted by lowercase letters.

UV-B portion of the spectrum. However, at the end of the experiment (Figure 6b) an opposite response, as compared to that of the beginning, was observed with UVR having a stimulatory effect (especially in the UV-B region) on HBP regardless the radiation treatments. Thus in Figure 6b, BWFs are represented as enhancement instead of inhibition. The samples acclimated to +UVR in the future condition were in general the most enhanced, displaying the largest differences with other treatments in the UV-A region.

There were significant short-term effects of solar UVR on HBP (i.e., comparing samples receiving UVR + PAR—under WG280 filter, and only PAR—i.e. under GG400 filter) for both environmental conditions (i.e. present and future) at the beginning of the experiment (Figure 7a). The observed UVR inhibition was significantly lower (*t*-test, $p < 0.05$) under the present (53.36 ± 5.51%) than under the future (73.92 ± 5.31%) environmental conditions. There was no significant interactive effect among solar short-term UVR exposure, acclimation to solar radiation and environmental conditions at the end of the acclimation phase (Table 2). However, at the end of the experiment, the bacterioplankton response reversed completely, having higher HBP in samples receiving UVR (i.e. under WG280) than when receiving only PAR (i.e. under GG400) for the present conditions (Figure 7b). The same trend was observed in samples under the future conditions although this was not significant.

Bacterial growth

Bacterial abundance had an initial mean value of 2.46×10^5 cells ml^{-1}. Results from ANOVAs showed interactive effects of the radiation acclimation × environmental conditions on mean bacterial growth rates (Table 2). In the future conditions, there was a lag-phase of the bacterial growth under +UVR, so the bacterial growth rate was calculated on three days, whereas under −UVR the lag-phase was absent and therefore bacterial growth rate was calculated on 4 days. The rates were significantly lower under the present than under the future condition (Figure 8); moreover, under this later condition bacterial growth rates were significantly lower in samples acclimated to +UVR than under −UVR. This led to a lower bacterial abundance under the present (mean value of present under +UVR and −UVR: $3.08 \times 10^5 \pm 7.81 \times 10^4$ cells ml^{-1}) than under the future conditions. Also, under the future conditions, bacterial abundance was lower under +UVR ($6.97 \times 10^5 \pm 2.03 \times 10^5$ cells ml^{-1}) than under −UVR ($1.63 \times 10^6 \pm 1.83 \times 10^5$ cells ml^{-1}).

Discussion

In this study, we assessed the short- (hours) and mid-term (days) effects of solar UVR, before and after acclimation to two solar radiation conditions (i.e. + UVR, and –UVR), comparing present with future conditions (i.e. scenario of increased nutrients and lower pH) on both, phyto- and bacterioplankton from Patagonian coastal waters, using as a model ecosystem the Chubut river estuary. Our experiments were carried out during summer, which is generally considered the post-bloom condition for phytoplankton in mid-latitude coastal Patagonian waters (Villafañe *et al.*, 2004). Summer conditions in our study site are extreme for planktonic organisms, as they are exposed to the highest temperatures and radiation levels (Helbling *et al.*, 2010). Moreover, the characteristic strong winds of this period carry continental dust which in addition to the input of nutrients

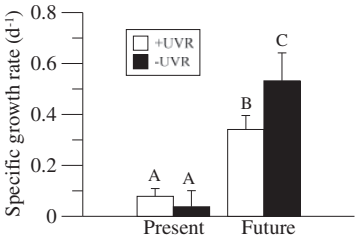

Figure 8. Specific growth rates (d^{-1}) of bacterioplankton acclimated to +UVR and −UVR under present and future environmental conditions. The values are the mean and the s.d. ($n = 3$). Significant differences among treatments are denoted by capital letters.

carried by the river (due to agricultural use of land, Helbling *et al.*, 1992) affect the chemical environment and thus the responses of planktonic communities to different variables (Marcoval *et al.*, 2008). Therefore, the conditions imposed in our experiments represent the worst future case scenario for the variables used in our study.

In the phytoplankton community, the interaction of variables considered in the future cluster (i.e. increase in nutrients and acidification) with UVR led to significant changes towards smaller diatom cells (Figure 5), with a decrease in the photochemical inhibition as the acclimation progressed (Figure 2), resulting in higher photosynthetic carbon fixation rates (Figure 4). These results agree with previous studies (e.g. Mostajir *et al.*, 1999) that showed a decrease in cell size under UVR exposure. Also, the decrease of the inhibition of Φ_{PSII} as the acclimation progressed, observed in both cluster conditions (Figure 2) has been previously documented for tropical phytoplankton communities (Villafañe *et al.*, 2014) and for several species of diatoms and dinoflagellates (Marcoval *et al.*, 2007). Furthermore, our results also coincide with a previous cluster experiment (Villafañe *et al.*, 2015) carried out by our group, where it was observed that increased nutrients and acidification resulted in an increase of carbon fixation rates as the acclimation progressed. An increase in CO_2 availability, associated with a decrease in pH, could result in down regulation of the cell carbon concentrating mechanisms, reducing the energy costs of carbon incorporation (Raven, 1991) and hence, in the absence of nutrient limitation, productivity would increase. In our short-term exposures it was also observed that samples acclimated to +UVR had higher carbon incorporation than those acclimated to −UVR when they were exposed to UVR (Figures 3 and 4), although some UVR impact was still observed. Thus, the acclimation conditions overall increased the phytoplankton performance as seen in another study (Villafañe *et al.*, 2015), resulting in acclimated cells and change in species composition (Figure 5) that can better cope with solar UVR and the imposed future conditions.

In the case of bacterioplankton, there was a clear inhibition of HBP due to UVR at the beginning of our experiments (Figures 6 and 7) and the initial BWF_{bact} agreed with previous ones obtained by Wilhelm and Smith (2000). However, at the end of the experiment, the bacterioplankton response reversed completely and HBP was enhanced under UVR exposure, especially in the present cluster condition (Figure 7b). This trend of enhancement of HBP was also observed in the future cluster condition although it was not significant. It is important to note that the different clusters had a significant impact on bacteria growth (Figure 8) which was increased in the future condition. However, since we quantified net bacterial growth, we cannot rule out changes in bacterivory or virus lysis due to the experimental treatments (McKie-Krisberg and Sanders, 2014; Motegi *et al.*, 2015) as a potential influence on bacterial community development. Even though at the end of the experiment the HBP per cell was rather similar among the environmental conditions (Figure 7b), the total HBP was significantly higher in the future condition than in the present, because of the higher amount of cells in the former. Despite the well described direct negative effects of UVR on several bacterioplankton cell targets (e.g. DNA—see review of Ruiz-González *et al.*, 2013) it is also important to consider the indirect effects caused by phytoplankton or by photolysis of DOM (Wilhelm and Smith, 2000). Excretion of organic carbon by phytoplankton (EOC) can be stimulated by UVR as a mechanism of reduction of algal physiological stress (Carrillo *et al.*, 2008), and this form of carbon is preferred than others sources of carbon by bacterioplankton (Kritzberg *et al.*, 2005). Thus, changes in EOC and/or photolysis of recalcitrant DOM into smaller molecules might have more important effects on the bacterioplankton metabolism than the direct UVR effects. Therefore, and although in our experimental approach we did not focus on the indirect effects of DOM or EOC on UVR sensitivity and its utilization by bacteria, one of the possible causes of the beneficial effects of UVR on bacteria at the end of the acclimation period might be due to the release of EOC by phytoplankton (especially in the future condition) as shown in other studies (Carrillo *et al.*, 2015). Unfortunately, logistic problems precluded us to obtain data on EOC in our experiments.

One of our main findings about the responses of bacteria over mid-term periods refers to the stimulation of their growth under future conditions. Acidification has been found to stimulate bacterial growth (Grossart *et al.*, 2006) by increasing the efficiency of extracellular enzymes such as leucine aminopeptidase (Piontek *et al.*, 2013; Endres *et al.*, 2014) and the incorporation of free-aminoacids (Grossart *et al.*, 2006) which might contribute to increase the bacterial abundance. Also, a higher production of transparent exopolymer particles under elevated CO_2 conditions (Endres *et al.*, 2014) and nutrients (Galgani *et al.*, 2014) might contribute to the stimulation of bacterial growth. Thus, a higher availability of organic carbon sources, besides higher inorganic nutrient availability, might be an explanation for the stimulation on specific growth rates of the bacterioplankton community found under future conditions in our study. Part of the stimulation of the bacteria growth observed under future conditions might be also due to taxonomic changes in the bacterial community along the experiment due to UVR exposure (Manrique *et al.*, 2012) as well as nutrients and acidification (Baltar *et al.*, 2015).

Summarizing, our results show that future conditions do not completely mitigate the UVR negative effects on phytoplankton, but reversed the effects of this waveband on bacterioplankton along the experiment, although this latter response might be largely influenced by indirect effects of UVR. Extrapolating the results from a mid-term experiment to a gradual and long-term process such as ocean acidification, might led to some uncertainties. However, our short- and mid-term results show the initial steps of response trends of phyto- and bacterioplankton to future disturbances, helping us to understand the acclimation mechanisms and changes in trophic relationships of these organisms. Thus, under future conditions of global change, UVR would have a key role in shaping the plankton community structure towards smaller cells i.e. by a reduction in phytoplankton cell sizes and an

increase in bacterioplankton abundance. On the one hand, changes in phytoplankton size would influence the carbon flux by changing grazing rates of zooplankton which in turn would affect growth rates of secondary consumers. On the other hand, the EOC released from more productive phytoplankton, although sensitive to UVR, would be channeled into the microbial loop by less UVR-sensitive bacterioplankton with higher growth rates. This might enhance the microbial carbon pump, biochemically transforming simple organic compounds to more recalcitrant carbon forms, and transferring carbon to non-bioavailable carbon reservoir (Legendre *et al.*, 2015). Although our results provide a first line of evidence for the study site of potential shifts in the microbial loop functioning under the tested conditions, further studies considering indirect effects and trophic relationships should also be performed.

Acknowledgements

We thank A. Buma for helpful discussions about this article. We also thank M. Hernando, P. Bermejo and M. J. Cabrerizo for radiocarbon, nutrient and flow cytometry analyses, respectively. P. Carrillo and J.M. Medina-Sánchez provided materials for bacterial production and flow cytometry measurements. The Cooperativa Eléctrica y de Servicios de Rawson provided the building's infrastructure to carry out these experiments. We thank the comments and suggestions of two anonymous reviewers and the Editors that helped us to improve this article.

Funding

This work was supported by Agencia Nacional de Promoción Científica y Tecnológica—ANPCyT (PICT 2012-0271 and PICT 2013-0208), Consejo Nacional de Investigaciones Científicas y Técnicas y Fundación Playa Unión. This is Contribution N° 165 of Estación de Fotobiología Playa Unión.

References

Allgaier, M., Riebesell, U., Vogt, M., Thyrhaug, R., and Grossart, H. P. 2008. Coupling of heterotrophic bacteria to phytoplankton bloom development at different pCO_2 levels: a mesocosm study. Biogeosciences, 5: 1007–1022.

Baltar, F., Palovaara, J., Vila-Costa, M., Salazar, G., Calvo, E., Pelejero, C., Marrasé, C., *et al.* 2015. Response of rare, common and abundant bacterioplankton to anthropogenic perturbations in a Mediterranean coastal site. FEMS Microbiology Ecology, 91: pii: fiv058.

Boyd, P. W., Strzepek, R., Fu, F. X., and Hutchins, D. A. 2010. Environmental control of open-ocean phytoplankton groups: Now and in the future. Limnology and Oceanography, 55: 1353–1376.

Buma, A. G. J., Visser, R. J., Van de Poll, W., Villafañe, V. E., Janknegt, P. J., and Helbling, E. W. 2009. Wavelength-dependent xanthophyll cycle activity in marine microalgae exposed to natural ultraviolet radiation. European Journal of Phycology, 44: 515–524.

Burrell, T. J., Maas, E. W., Teesdale-Spittle, P., and Law, C. S. 2016. Assessing approaches to determine the effect of ocean acidification on bacterial processes. Biogeosciences, 13: 4379–4388.

Cai, W. J., Hu, X., Huang, W. J., Murrell, M. C., Lehrter, J. C., Lohrenz, S. E., Chou, W. C., *et al.* 2011. Acidification of subsurface coastal waters enhanced by eutrophication. Nature Geoscience, 4: 766–770.

Carrillo, P., Delgado-Molina, J. A., Medina-Sánchez, J. M., Bullejos, F. J., and Villar-Argaiz, M. 2008. Phosphorus inputs unmask negative effects of ultraviolet radiation on algae in a high mountain lake. Global Change Biology, 14: 423–439.

Carrillo, P., Medina-Sánchez, J. M., Durán, C., Herrera, G., Villafañe, V. E., and Helbling, E. W. 2015. Synergistic effects of UVR and simulated stratification on commensalistic algal-bacterial relationship in two optically contrasting oligotrophic Mediterranean lakes. Bioegeosciences, 12: 697–712.

Chen, H., Guan, W., Zeng, G., Li, P., and Chen, S. 2014. Alleviation of solar ultraviolet radiation (UVR)-induced photoinhibition in diatom *Chaetoceros curvisetus* by ocean acidification. Journal of the Marine Biological Association of the United Kingdom, 95: 661–667.

Cloern, J. E., Foster, S. Q., and Fleckner, A. E. 2014. Phytoplankton primary production in the world's estuarine-coastal ecosystems. Biogeosciences, 11: 2477–2501.

Crain, C. M., Kroeker, K., and Halpern, B. S. 2008. Interactive and cumulative effects of multiple human stressors in marine systems. Ecology Letters, 11: 1304–1315.

De Senerpont Domis, L. N., Elser, J. J., Gsell, A. S., Huszar, V. L. M., Ibelings, B. W., Jeppesen, E., Kosten, S., *et al.* 2013. Plankton dynamics under different climatic conditions in space and time. Freshwater Biology, 58: 463–482.

Depetris, P. J., Gaiero, D. M., Probst, J. L., Hartmann, J., and Kempe, S. 2005. Biogeochemical output and typology of rivers draining Patagonia's Atlantic seaboard. Journal of Coastal Research, 21: 835–844.

Domingues, R. B., Guerra, C. C., Barbosa, A. B., Brotas, V., and Galvao, H. M. 2014. Effects of ultraviolet radiation and CO_2 increase on winter phytoplankton assemblages in a temperate coastal lagoon. Journal of Plankton Research, 36: 672–684.

Doney, S. C., Fabry, V. J., Feely, R. A., and Kleypas, J. A. 2009. Ocean acidification: the other CO_2 problem. Annual Review of Marine Science, 1: 169–192.

Duarte, C. M., Hendriks, I. E., Moore, T. S., Olsen, Y. S., Steckbauer, A., Ramajo, L., Carstensen, J., *et al.* 2013. Is ocean acidification an open-ocean syndrome? Understanding anthropogenic impacts on seawater pH. Estuaries and Coasts, 36: 221–236.

Endres, S., Galgani, L., Riebesell, U., Schulz, K. G., and Engel, A. 2014. Stimulated bacterial growth under elevated pCO_2: Results from an off-shore mesocosm study. PLoS One, 9: e99228.

England, M. H., McGregor, S., Spence, P., Meehl, G. A., Timmermann, A., Cai, W., Gupta, A. S., *et al.* 2014. Recent intensification of wind-driven circulation in the Pacific and the ongoing warming hiatus. Nature Climate Change, 4: 222–227.

Galgani, L., Stolle, C., Endres, S., Schulz, K. G., and Engel, A. 2014. Effects of ocean acidification on the biogenic composition of the sea-surface microlayer: Results from a mesocosm study. Journal of Geophysical Research-Oceans, 119: 7911–7924.

Gao, K., Wu, Y., Li, G., Wu, H., Villafañe, V. E., and Helbling, E. W. 2007. Solar UV radiation drives CO_2 fixation in marine phytoplankton: A double-edged sword. Plant Physiology, 144: 54–59.

Gattuso, J. P., Gao, K., Lee, K., Rost, B., and Schulz, K. G. 2010. Approaches and tools to manipulate the carbonate chemistry. *In* Guide to Best Practices for Ocean Acidification Research and Data Reporting, pp. 41–52. Ed. by U. Riebesell, V. J. Fabry, L. Hansson, and J.-P. Gattuso. Publications Office of the European Union, Brussels.

Genty, B. E., Briantais, J. M., and Baker, N. R. 1989. The relationship between the quantum yield of photosynthetic electron transport and quenching of chlorophyll fluorescence. Biochimica et Biophysica Acta, 990: 87–92.

Grossart, H. P., Allgaier, M., Passow, U., and Riebesell, U. 2006. Testing the effect of CO_2 concentration on the dynamics of marine heterotrophic bacterioplankton. Limnology and Oceanography, 51: 1–11.

Häder, D. P., Williamson, C. E., Wängberg, S. A., Rautio, M., Rose, K. C., Gao, K., Helbling, E. W., *et al.* 2015. Effects of UV radiation on aquatic ecosystems and interactions with other environmental

factors. Photochemical and Photobiological Sciences, 14: 108–126.

Häder, D. P., Villafañe, V. E., Richter, P., and Helbling, E. W. 2015. Water parameters of the Chubut River and Andes lakes (Patagonia, Argentina), pp. 293–310. In Biological Sciences. Innvovations and dynamics. Ed. by R.P., Sinha, Richa and R. P. Rastogi. New India Publishing Agency, New Delhi, India.

Helbling, E. W., Banaszak, A. T., and Villafañe, V. E. 2015. Differential responses of two phytoplankton communities from the Chubut river estuary (Patagonia, Argentina) to the combination of UVR and elevated temperature. Estuaries and Coasts, 38: 1134–1146.

Helbling, E. W., Pérez, D. E., Medina, C. D., Lagunas, M. G., and Villafañe, V. E. 2010. Phytoplankton distribution and photosynthesis dynamics in the Chubut River estuary (Patagonia, Argentina) throughout tidal cycles. Limnology and Oceanography, 55: 55–65.

Helbling, E. W., Santamarina, J. M., and Villafañe, V. E. 1992. Chubut river estuary (Argentina): Estuarine variability under different conditions of river discharge. Revista de Biología Marina, 27: 73–90.

Holm-Hansen, O., and Helbling, E. W. 1995. Técnicas para la medición de la productividad primaria en el fitoplancton. *In* Manual de Métodos Ficológicos, pp. 329–350. Ed. by K. Alveal, M. E. Ferrario, E. C. Oliveira, and E. Sar. Universidad de Concepción, Concepción.

Holm-Hansen, O., Lorenzen, C. J., Holmes, R. W., and Strickland, J. D. H. 1965. Fluorometric determination of chlorophyll. Journal du Conseil permanent International pour l' Exploration de la Mer, 30: 3–15.

Holm-Hansen, O., and Riemann, B. 1978. Chlorophyll *a* determination: Improvements in methodology. Oikos, 30: 438–447.

IPCC 2013. Climate Change 2013. The Physical Science Basis, Cambridge University Press, New York, USA. 1535 pp.

Kritzberg, E. S., Cole, J. J., Pace, M. M., and Graneli, W. 2005. Does autochthonous primary production drive variability in bacterial metabolism and growth efficiency in lakes dominated by terrestrial C inputs?. Aquatic Microbial Ecology, 38: 103–111.

Legendre, L., Rivkin, R. B., Weinbauer, M. G., Guidi, L., and Uitz, J. 2015. The microbial carbon pump concept: Potential biogeochemical significance in the globally changing ocean. Progress in Oceanography, 134: 432–450.

Mahowald, N., Lindsay, K., Rothenberg, D., Doney, S. C., Moore, J. K., Thornton, P., Randerson, J. T., *et al.* 2011. Desert dust and anthropogenic aerosol interactions in the Community Climate System Model coupled-carbon-climate model. Biogeosciences, 8: 387–414.

Manrique, J. M., Calvo, A. Y., Halac, S. R., Villafañe, V. E., Jones, L. R., and Helbling, E. W. 2012. Effects of UV radiation on the taxonomic composition of natural bacterioplankton communities from Bahia Engaño (Patagonia, Argentina). Journal of Photochemistry and Photobiology B-Biology, 117: 171–178.

Marcoval, M. A., Villafañe, V. E., and Helbling, E. W. 2007. Interactive effects of ultraviolet radiation and nutrient addition on growth and photosynthesis performance of four species of marine phytoplankton. Journal of Photochemistry and Photobiology, B: Biology, 89: 78–87.

Marcoval, M. A., Villafañe, V. E., and Helbling, E. W. 2008. Combined effects of solar ultraviolet radiation and nutrients addition on growth, biomass and taxonomic composition of coastal marine phytoplankton communities of Patagonia. Journal of Photochemistry and Photobiology, B: Biology, 91: 157–166.

McKie-Krisberg, Z. M., and Sanders, R. W. 2014. Phagotrophy by the picoeukaryotic green algae *Micromonas*: Implications for Artic Oceans. ISME Journal, 8: 1953–1961.

Medina-Sánchez, J. M., Villar-Argaiz, M., and Carrillo, P. 2002. Modulation of the bacterial response to spectral solar radiation by algae and limiting nutrients. Freshwater Biology, 47: 2191–2204.

Medina-Sánchez, J. M., Villar-Argaiz, M., and Carrillo, P. 2006. Solar radiation - nutrient interaction enhances the resource and predation algal control on bacterioplankton: a short-term experimental study. Limnology and Oceanography, 51: 913–924.

Mercado, J. M., Sobrino, C., Neale, P. J., Segovia, M., Reul, A., Amorim, A. L., Carrillo, P., *et al.* 2014. Effect of CO_2, nutrients and light on coastal plankton. II. Metabolic rates. Aquatic Biology, 22: 43–57.

Mostajir, B., Sime-Ngando, T., Demers, S., Belzile, C., Roy, S., Gosselin, M., Chanut, J. P., *et al.* 1999. Ecological implications of changes in cell size and photosynthetic capacity of marine Prymnesiophyceae induced by ultraviolet-B radiation. Marine Ecology Progress Series, 187: 89–100.

Motegi, C., Kaiser, K., Benner, R., and Weinbauer, M. G. 2015. Effect of P-limitation on prokaryotic and viral production in surface waters of the Northwestern Mediterranean Sea. Journal of Plankton Research, 37: 16–20.

Neale, P. J. 2000. Spectral weighting functions for quantifying effects of UV radiation in marine ecosystems. *In* The effects of UV radiation on marine ecosystems, pp. 72–100. Ed. by S. J. De Mora, S. Demers, and M. Vernet. Cambridge University Press, Cambridge.

Neale, P. J., and Kieber, D. J. 2000. Assesing biological and chemical effects of UV in the marine environment: Spectral weighting functions. *In* Causes and environmental implications of increased UV-B radiation, pp. 61–83. Ed. by R. E. Hester, and R. M. Harrison. The Royal Society of Chemistry, Cambridge.

Ogbebo, F. E., and Ochs, C. 2008. Bacterioplankton and phytoplankton production rates compared at different levels of solar ultraviolet radiation and limiting nutrient ratios. Journal of Plankton Research, 30: 1271–1284.

Piontek, J., Borchard, C., Sperling, M., Schulz, K. G., Riebesell, U., and Engel, A. 2013. Response of bacterioplankton activity in an Arctic fjord system to elevated pCO_2: results from a mesocosm perturbation study. Biogeosciences, 10: 297–314.

Raven, J. A. 1991. Physiology of inorganic C adquisition and implications for resource use efficiency by marine phytoplankton: Relation to increased CO_2 and temperature. Plant, Cell and Environment, 14: 779–794.

Ruiz-González, C., Simó, R., Sommaruga, R., and Gasol, J. M. 2013. Away from darkness: A review on the effects of solar radiation on heterotrophic bacterioplankton activity. Frontiers in Microbiology - Aquatic Microbiology, 4: 1–24.

Rundel, R. D. 1983. Action spectra and estimation of biologically effective UV radiation. Physiologia Plantarum, 58: 360–366.

Sabine, C. L., Feely, R. A., Gruber, N., Key, R. M., Lee, K., Bullister, J. L., Wanninkhof, R., *et al.* 2004. The oceanic sink for anthropogenic CO_2. Science, 305: 367–371.

Satoh, A., Kurano, N., and Miyachi, S. 2001. Inhibition of photosynthesis by intracellular carbonic anhydrase in microalgae under excess concentrations of CO_2. Photosynthesis Research, 68: 215–224.

Scavia, D., Field, J. C., Boesch, D. F., Buddemeier, R. W., Burkett, V., Cayan, D. R., Fogarty, M., *et al.* 2002. Climate change impacts on U. S. coastal and marine ecosystems. Estuaries, 25: 149–164.

Shi, D., Xu, Y., and Morel, F. M. M. 2009. Effects of the pH/pCO_2 control method on medium chemistry and phytoplankton growth. Biogeosciences, 6: 1199–1207.

Simon, M., and Azam, F. 1989. Protein-content and protein-synthesis rates of planktonic marine-bacteria. Marine Ecology Progress Series, 51: 201–213.

Skewgar, E., Boersma, P. D., Harris, G., and Caille, G. 2007. Sustainability: Anchovy fishery threat to Patagonian Ecosystem. Science, 315: 45.

Smith, D. C., and Azam, F. 1992. A simple, economical method for measuring bacterial protein synthesis rates in seawater using tritiated-leucine. Marine Microbial Food Webs, 6: 107–114.

Sobrino, C., Ward, M. L., and Neale, P. J. 2008. Acclimation to elevated carbon dioxide and ultraviolet radiation in the diatom *Thalassiosira pseudonana*: Effects on growth, photosynthesis, and spectral sensitivity of photoinhibition. Limnology and Oceanography, 53: 494–505.

Strickland, J. D. H., and Parsons, T. R. 1972. A practical handbook of seawater analysis. Fisheries Research Board of Canada, Bull, 167: 1–310.

Villafañe, V. E., Barbieri, E. S., and Helbling, E. W. 2004. Annual patterns of ultraviolet radiation effects on temperate marine phytoplankton off Patagonia, Argentina. Journal of Plankton Research, 26: 167–174.

Villafañe, V. E., Erzinger, G. S., Strauch, S. M., and Helbling, E. W. 2014. Photochemical activity of PSII of tropical phytoplankton communities of Southern Brazil exposed to solar radiation and nutrient addition. Journal of Experimental Marine Biology and Ecology, 459: 199–207.

Villafañe, V. E., Sundbäck, K., Figueroa, F. L., and Helbling, E. W. 2003. Photosynthesis in the aquatic environment as affected by UVR. In UV effects in aquatic organisms and ecosystems, pp. 357–397. Ed. by E. W. Helbling, and H. E. Zagarese. Royal Society of Chemistry, Cambridge.

Villafañe, V. E., Valiñas, M. S., Cabrerizo, M. J., and Helbling, E. W. 2015. Physio-ecological responses of Patagonian coastal marine phytoplankton in a scenario of global change: Role of acidification, nutrients and solar UVR. Marine Chemistry, 177: 411–420.

Wilhelm, S. W., and Smith, R. E. H. 2000. Bacterial carbon production in Lake Erie is influenced by viruses and solar radiation. Canadian Journal of Fisheries and Aquatic Sciences, 57: 317–326.

Yates, K. K., DuFore, C. M., and Robbins, L. L. 2013, Chemical and biological consequences of using carbon dioxide versus acid additions in ocean acidification experiments: U.S. Geological Survey Scientific Investigations Report 2012-5063, 17 p.

Zar, J. H. 1999. Biostatistical Analysis, Prentice Hall, Englewood Cliffs, NJ.

Zubkov, M., Burkill, P. H., and Topping, J. N. 2007. Flow cytometric enumeration of DNA-stained oceanic planktonic protists. Journal of Plankton Research, 29: 79–86.

Zubkov, M. V., and Burkill, P. H. 2006. Syringe pumped high speed flow cytometry of oceanic phytoplankton. Cytometry Part A, 69A: 1010–1019.

Handling editor: Shubha Sathyendranath